



## Improve Synthesis of Iron Oxide Nanorode with Hydrothermal Method

M. Aghazadeh<sup>1</sup>, Fatemeh. Aghazadeh<sup>2\*</sup>

<sup>1</sup>Department of Physics, Faculty of Science, Islamic Azad University, Karaj Branch, Karaj, Iran

<sup>2</sup>Department of Chemistry, Faculty of Science, Islamic Azad University, Karaj Branch, Karaj, Iran.

(Received 13 Feb. 2013; Final version received 20 Jun. 2013)

---

### Abstract

Maghemite and magnetite nanoparticles and nanorode are now losing interests in the field of nanobiotechnology and pharmaceutical for their applications. This paper reports on a hydrothermal process for the synthesis of  $Fe_2O_3$  in the  $\gamma$ -phases nanorodes, when the hydrothermal temperature was  $100^\circ C$ . The uniqueness of the method lies in the use of ferrous ammonium sulphate, hexamine was added as the stabilizer and hydrolyzing agents. The crystal structure, shape particle and magnetic properties of the samples were determined by X-ray diffraction (XRD) and Transmission electron microscopy (TEM) and magnetometer (AGFM), respectively. The particle size was 60nm and length in the range of 300nm. The magnetic behavior of the particles was like the typical behavior of superparamagnetic particles, so smaller particles can improve the magnetic properties and decreasing the coercivity.

**Keywords:** *Magnetic materials, Hydrothermal method,  $Fe_2O_3$  nanorode.*

---

### Introduction

Magnetic iron oxides have always been attractive to scientists due to great potential applications in different areas. Iron oxide nanoparticles with their wide range of applications have always attracted a lot of interest. Magnetic iron oxides like maghemite and magnetite have been used for many biomedical applications such as targeted drug delivery, separation of biomedical

products, cell separation, in cancer therapy, magnetic induced hyperthermia, MRI contrast agent, immunomagnetic separation IMC and others. The magnetic properties of maghemite play an important role in different applications of health care. A large number of materials in bulk as well as in the form of nanoparticles have been created for a variety of photochemical and photo electrochemical applications [1-7].

---

\*Corresponding author: Fatemeh Aghazadeh, Department of Chemistry, Islamic Azad University, Karaj Branch, Karaj, Iran. E-mail: aghazadeh\_ch@yahoo.com. Tel.: 0098-26-34316125.

To design any application for such nanoparticles, it is necessary to find a synthesis route which provides good control on particle size with narrow size distribution in addition to being quick and low cost. Each application requires specific material properties. The size and the shape of the magnetite nanocrystals are important for their strong influence on the magnetic behavior of the particles. The magnetic single-domain ranges of size from 30 to 120 nm.

For crystals smaller than 30 nm the magnetization spontaneously changes its direction because of thermal fluctuations. These grains are superparamagnetic. Crystals larger than 120 nm are multi-domain and have lower remanent magnetization than single-domain crystals. In general, the more elongated the crystals, the better constrained is the direction of the magnetic induction, particularly if the elongation and the easily magnetisable direction are parallel to each other [8]. Gamma  $\text{Fe}_2\text{O}_3$  (maghemite) is the ferromagnetic cubic form of Fe (III) oxide and it differs from the inverse spinel structure of magnetite through vacancies on the cation sublattice.

Maghemite has the same crystalline structure like magnetite. Main distinct features of maghemite are the presence of vacancies in Fe position with symmetry reduction. Gamma and epsilon type  $\text{Fe}_2\text{O}_3$  are ferromagnetic, alpha- $\text{Fe}_2\text{O}_3$  is a canted antiferromagnetic while beta type  $\text{Fe}_2\text{O}_3$  is a paramagnetic material [7].

Various methods for preparation of iron oxide nanoparticles, such as oxidation of iron nanoparticles [9], spray pyrolysis [10-11], microwave irradiation [12]; electrodepositing [13], co-precipitation [14, 15] and hydrothermal [16-17] have been reported in the literature [18-20].

The hydrothermal method used hydrolyzing agents such as sodium hydroxide, sodium hydroxide + hexamine, ammonia, ammonia + formaldehyde [21]. Hexamine is known to assist anisotropic growth of metal oxides and the same is also found to be true for magnetite nanosynthesis. It elucidates the role of hexamine and other precursors in the formation of magnetite nanorods by the hydrothermal route and their stoichiometry [21-22]. Hydrothermal synthesis of iron oxide nanorod can be performed by using different precursors under various temperature–pressure conditions. For the first time, we report the hydrothermal synthesis of maghemite nanorode by using ferrous ammonium sulfate (FAS), as the source of ferric ions and hexamine is known stabilizer and hydrolyzing agents. We are also studied the role of hexamine in the formation of maghemite nanorode by the hydrothermal method.

## **Experimental**

For the synthesis of Iron oxide nanorode, ferrous ammonium sulphate (FAS) (analytical grade, Merck, Germany) was used as

the source of ferrous ions and hexamine (analytical grade, Merck, Germany) was used as a stabilizer and hydrolyzing agent. A typical synthesis involved 20 ml, 0.01 M solution of FAS, mixed with 3g Hexamine in 100 ml water. The mixed solution was put in a 100 ml Teflon lined reaction vessel autoclave. The reaction was carried out at 100 oC, for duration of 1.5 hours. After the completion of reaction a brownish precipitate was formed. The precipitate was washed with water and was finally dried in oven (time= 5 hr. and temperature = 100° C).

The structure and phase purity of as-synthesized samples were examined by using powder X-ray diffraction (Philips, PW-3710) with Cu  $k\alpha$  (wavelength = 1.54056Å and filter wide range of Bragg's angles or scan speed: 20°<2 $\theta$ <60°, XRD scan speed Standard 10, depending on measurement conditions) radiation as the source of X-rays. The size and the morphology of the particles were investigated by using transmission electron microscope (TEM), model ZEISS, CEM 902A operating at 100 KV. Magnetic measurements were carried out by using an alternating gradient force magnetometer (AGFM).

## Results and discussion

Hydrothermal treatment of iron salt could generate iron oxides when the applied conditions are appropriate. The hydrothermal preparation of  $\gamma$ -Fe<sub>2</sub>O<sub>3</sub> from amorphous iron

(III) hydroxide was studied in the temperature 100oC.

The first in situ investigation of the rate of crystallization of amorphous iron (III) hydroxide to  $\gamma$ -Fe<sub>2</sub>O<sub>3</sub> was made at hydrothermal conditions (T=100°C, time=1.5 hr.). The particle size was controlled by means of the coexistence effects of sulfate ions. For the synthesis of Iron oxide nanorode, ferrous ammonium sulphate (FAS) (in conjugation with FeCl<sub>3</sub>) which helps maintain the stability of Fe<sup>+2</sup> state in the reaction sequence thereby controlling the phase formation and the hexamine was added as the stabilizer, hydrolyzing agents, ferrous sulphate and hexamine as raw materials. However, a partial Fe(OH)<sub>3</sub> was linked together by the completing effect of the hexamine, resulting in the bonding of partial Fe<sub>2</sub>O<sub>3</sub> nonorodes. The mechanism of formation is as follows. In the formation process of Fe<sub>2</sub>O<sub>3</sub>, Fe<sup>2+</sup> hydrolyzed in the solution to form a Fe(OH)<sub>3</sub> and so, the dehydrates around 100°C.

The structure of  $\gamma$ -Fe<sub>2</sub>O<sub>3</sub> is similar to that of Fe<sub>3</sub>O<sub>4</sub>, but with cation vacancies at the octahedral site of the spinel lattice [23, 24]. The ordering of these vacancies can occur in different forms leading to different crystal symmetries. It has been shown that the cation vacancy distribution depend on the preparation method of  $\gamma$ -Fe<sub>2</sub>O<sub>3</sub>. The low temperature methods of synthesis usually lead to the formation of disordered phase.

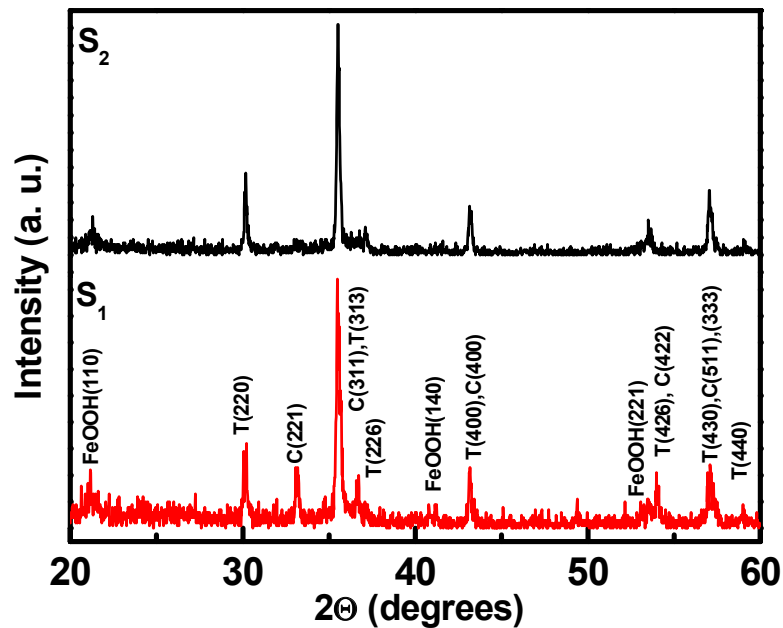
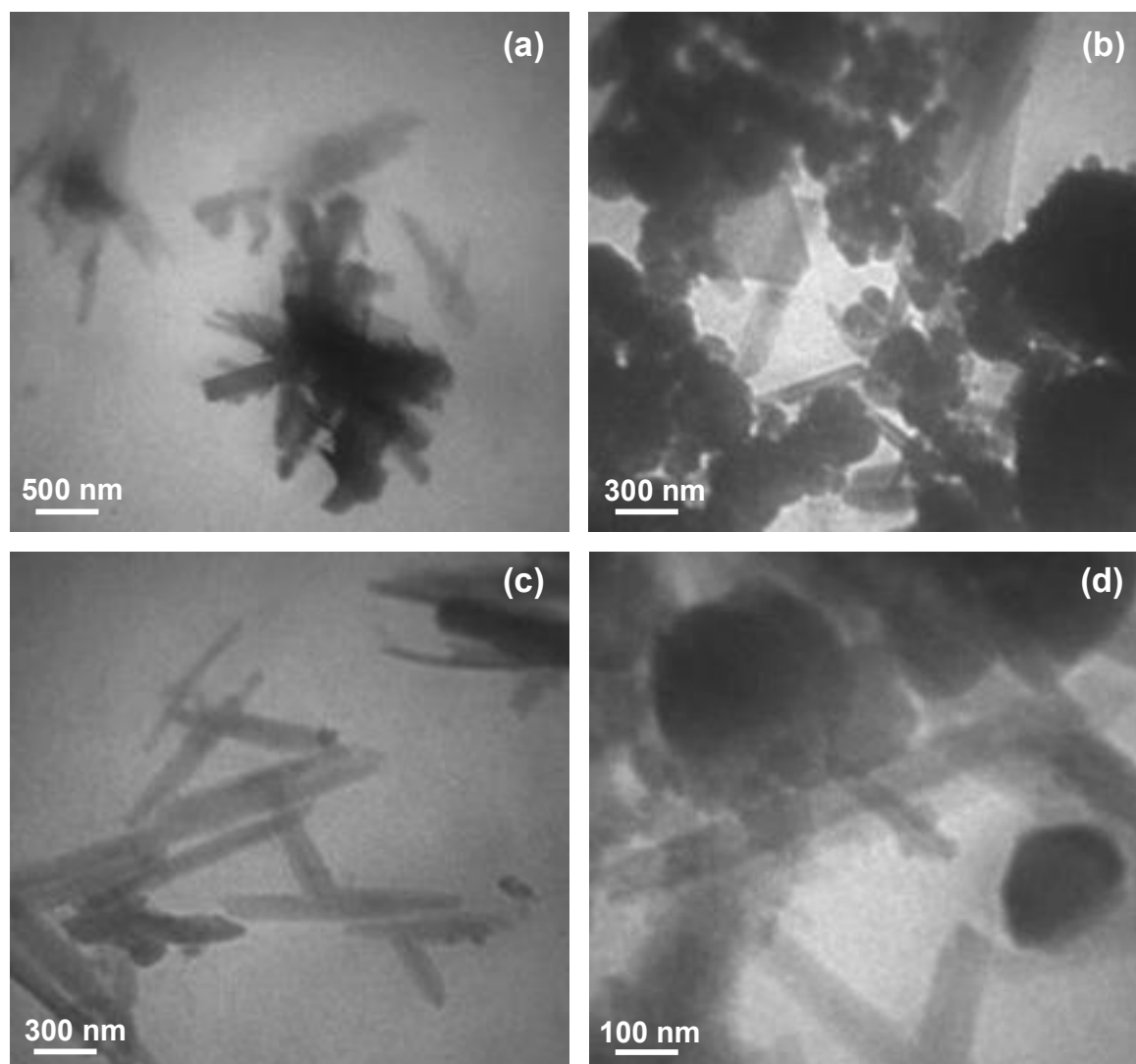


Figure 1. XRD pattern of samples  $S_1$  and  $S_2$ .

The phase purity and crystal structure of the synthesized nanorod were investigated by powder X-ray diffraction (XRD), as shown in Figure 1. As it could be observed, the samples are well crystalline but the structure and phases vary in these samples, depending on the reaction conditions. In samples  $S_1$  and  $S_2$ , where the reaction time increases from 1.5 hours, the phase purity improves drastically, showing peaks attributed to the tetragonal  $\gamma$ - $\text{Fe}_2\text{O}_3$  phase. TEM micrographs (Figure 2) confirmed that

sample  $S_2$  consists of elongated round shaped particles, with an average width of 60nm and length in the range of 300nm.  $\gamma$ - $\text{Fe}_2\text{O}_3$  nanorod with similar morphology (elongated) was also reported by Fang et al. [25]. Sample  $S_1$ , on the other hand, contained particles which look larger and of arbitrary shapes with some elongated particles formed. This is in good agreement with XRD results which showed that  $S_2$  was in more pure form and therefore of better reaction time.



**Figure 2.** TEM micrographs of samples  $S_1$  (a, b) and  $S_2$  (c, d).

Figure 3 shows the magnetization as a function of magnetic field ( $M$  vs.  $H$ ) recorded at 300 K. Both the samples show a measurable hysteresis even though the coercivity ( $H_C$ ) is very small, 17.1 Oe in  $S_1$  and 71.6 Oe in  $S_2$ . The saturate magnetization is higher in  $S_2$  as the particles have grown mix large and spherical in this sample. The coercivity of the nanorode

increases with increasing particle size. In both the samples the magnetization rapidly increases with applied field but in  $S_1$  hardly reaches saturation even in 8 KOe applied field whereas the magnetization of  $S_2$  reaches saturation in about 6 KOe. The magnetic behavior of the samples is similar to that of superparamagnetic nanorodes.

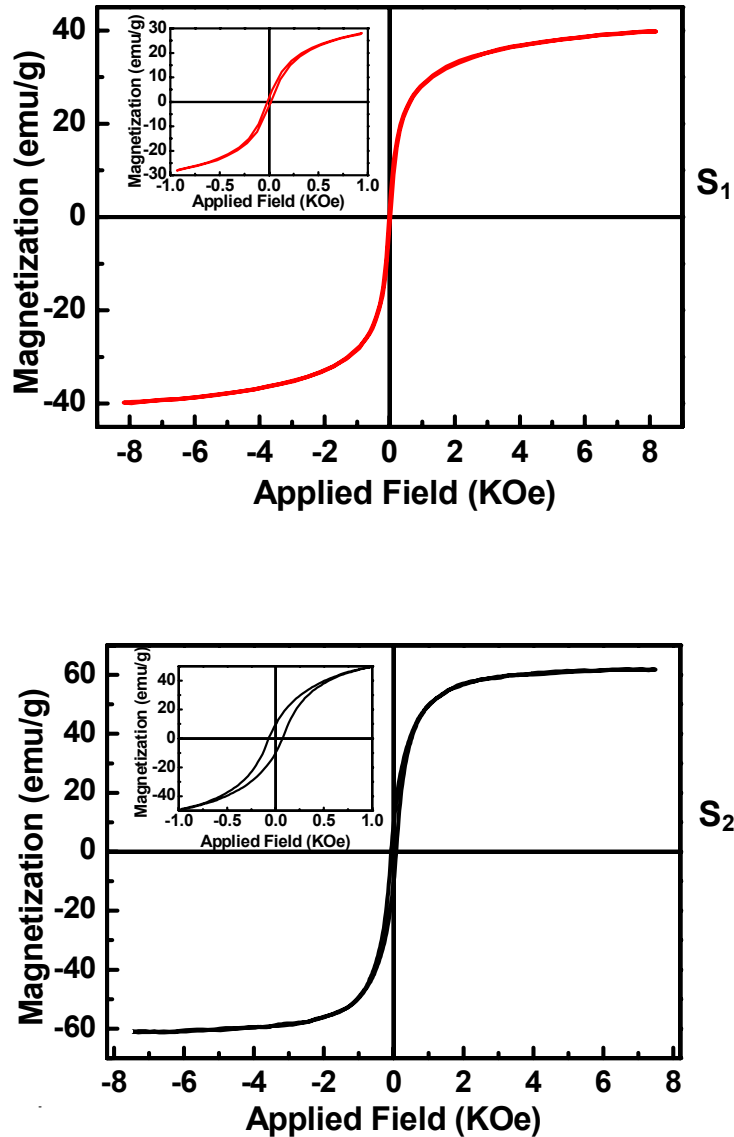


**Figure 3.** Magnetization ( $M$ ) versus applied magnetic field ( $H$ ) isotherms at room temperature for samples  $S_1$  and  $S_2$ .

### Conclusions

It was shown that FAS and hexamine can be used as a precursor for the hydrothermal synthesis of  $\gamma$ - $\text{Fe}_2\text{O}_3$  nanorods. The nanoparticles were with needle like shape. In samples, where the reaction time increases from 1.5 hours, the phase purity improves drastically, showing peaks attributed

to the tetragonal  $\gamma$ - $\text{Fe}_2\text{O}_3$  phase. The particle size was 60nm in width and 300nm in length. Therefore, both the samples show a measurable hysteresis even though the coercivity (HC) is very small, 17.1 Oe in  $S_1$  and 71.6 Oe in  $S_2$ . The saturate magnetization is higher in  $S_2$  as the particles have grown larger in this sample.

The magnetic behavior of the particles was like the typical behavior of superparamagnetic particles, though achieving smaller particles can improve the magnetic properties of the particles namely decreasing the coercivity.

## References

- [1] W. Wu, Q. He, C. Jiang *Nanoscale Res. Lett.*, 3 397 (2008).
- [2] S. Laurent, D. Forge, M. Port, A. Roch, A. Robic, A. Vander, *Chem. Rev.*, 108, 2064 (2008).
- [3] A. K. Gupta, M. Gupta. *Biomaterials*, 26, 3995 (2005).
- [4] P. Tartaj, M.P. Morales, T. González-Carreño, S. Veintemillas-Verdaguer, C.J. Serna, *J. Magn. Magn. Mater.*, 28, 290 (2005).
- [5] T. Neuberger, B. Schöpf, H. Hofmann, *J. Magn. Magn. Mater.*, 293, 483 (2005).
- [6] T.k.Indira, P.K.Lakshmi, *International Journal of Pharmaceutical sciences and nanotechnology*, 3, 1035 (2010).
- [7] M.Chirita, I. Groztesca, *Chem. Bull.*, 54, 1 (2009).
- [8] I.N Kosa, D.C. Nagy, M. Posfai, *Eur. J. Mineral.*, 21, 293 (2009).
- [9] T. Hyeon, S.S. Lee, J. Park, Y. Chung, *J. Am. Chem. Soc.*, 123, 12798 (2001).
- [10] R.F.C. Marqus, A.F.R. Rodriguez, J.A.H. Coaquira, *Hyperfine Interactions*, 189, 159 (2009).
- [11] D. Li, W.Y. Teoh, C. Selomulya, R.C. woodward, *J. Mater. Chem.*, 17, 4876 (2007).
- [12] V. Sreeja, P.A. Joy, *Mater. Res. Bulletin*, 42, 1570 (2007).
- [13] H. Park, P. Ayala, M.A. Deshusses, A. Mulchandani, *Chem. Eng. J.*, 139, 208 (2008).
- [14] S.J. Lee, J.R. Jeong, S.C. Shin, *J. Magn. Magn. Mater.*, 282, 147 (2004).
- [15] J. Drbohlavova, R. Hrdy, V. Adams, R. Kizek, O.Schneeweiss, J. Hubalek, *Sensors*, 9, 2352 (2009).
- [16] O. Horner, S. Neveu, S. de Montredon, *Nanoparticle Res.* 11, 1247 (2009).
- [17] H. Zhu, D. Yang, L. Zhu, H. Yang, D. Jin, K. Yao, *J. Mater. Sci.*, 42, 9205 (2007).
- [18] G.Demazeau, *Journal of Materials Science*, 43(7), 2104 (2008).
- [19] H. Cui, Y. Feng, W. Ren, T.Zeng, H.Lv, Y. Feipan, *Récent Patents on Nanotechnology*, 3, 32 (2009).
- [20] M.A. Willard, L.K. Kurihara, E.E. Carpenter, S. Calvin, V.G. Harris, *Inter. Mater. Rev.*, 49, 129 (2004).
- [21] H. Singh, S. Bhagwat, S. Jouen, B. Lefezb, A.A. Athawale, B. Hannoyer, S.Ogale, *J.Phys. Chem.Chem.Phys.*, 12 (13), 3246 (2010).
- [22] S.V.Bhagwat, S.Jouen, D.C. Kundaliya, H.Singh, T.Jagadale, A.A.Athawale, S.Loffland, B.Hannoyer, S.B. Ogale, *Journal of Nanoscience and Nanotechnology*, 910, 5823 (2009).
- [23] J.E. Jørgensen, L. Mosegaard, L.E. Thomsen, T.R. Jensen, J.C. Hanson, *J. Solid Stat. Chem.*, 180, 180 (2007).
- [24] T.J. Bastow, A. Trinchi, M.R. Hill, R.

Harris, *J. Magn. Magn. Mater.*, 321, 2677  
(2009).

[25] J. Fang, A. Kumbhar, W.L. Zhou, K.L.  
Stokes, *Mater. Res. Bull.*, 38, 461 (2003).